Short-range order in bulk Zr- and Hf-based amorphous alloys

L.C. Damonte [a],*, L. Mendoza-Zélis [a], J. Eckert [b]

[a] *Departamento de Física, Facultad de Ciencias Exactas, Universidad Nacional de La Plata, C.C.67, 1900 La Plata, Argentina*
[b] *IFW Dresden, Institut für Metallische Werkstoffe, Postfach 270016, 01171 Dresden, Germany*

Abstract

The local order in mechanically alloyed $Hf_{65}Al_{7.5}Cu_{17.5}Ni_{10}$ and $Zr_{65}Al_{7.5}Cu_{17.5}Ni_{10}$ amorphous alloys was studied by means of perturbed angular correlation measurements. The amorphous state of the starting material was confirmed by X-ray diffraction. Differential scanning calorimetry analysis showed the existence of an extended supercooled liquid region. Two exothermic effects, indicating a two-step crystallization process, were also observed. Perturbed angular correlation measurements indicated similar short-range order in the supercooled liquid state and in the starting amorphous state. The evolution of short-range order with annealing temperature was also studied ,being the intermediate and final phases characterized by this hyperfine technique. © 2000 Elsevier Science S.A. All rights reserved.

Keywords: Short-range order; Amorphous alloys; Angular correlation

1. Introduction

The metallic alloys $Hf_{65}Al_{7.5}Cu_{17.5}Ni_{10}$ and $Zr_{65}Al_{7.5}Cu_{17.5}Ni_{10}$ belong to a new class of amorphous materials that exhibit interesting and unique properties [1–4]. Among these properties, the existence of a wide supercooled liquid region (SLR), $\Delta T_x = T_x - T_g$, of about 50 K, provides the possibility of studying different structural and electronic properties of the amorphous state over an extended temperature range. The production of these new amorphous materials by conventional techniques does not require high cooling rates [1–3], thus enabling the production of bulk samples. Mechanical alloying from crystalline elemental powders was also successfully applied to produce these amorphous alloys [4–6].

Since the pioneering work of the groups of Johnson and Inoue on casting of bulk glasses and after the production of amorphous Zr–Ti–Cu–Ni and Zr–Al–Cu–Ni alloys by mechanical alloying [4–6], a great amount of work has been done on these Zr-based metallic alloys. These mainly deal with different preparation methods, composition and stability of amorphous alloys. However, the characteristics of their microstructure, relaxation and crystallization behavior were not much investigated. In the Zr–Cu–Ni–Be–Ti system, a complicated microstructural relaxation associated with phase separation in the SLR was established by the use of a variety of techniques. Also small-angle neutron scattering was applied to investigate the kinetics of crystallization and phase separation in Zr–Cu–Ni–Be–Ti alloy [7–9].

The electric field gradient (EFG)-sensitive techniques have already demonstrated their capability in the analysis of the local atomic order in amorphous alloys [10–15]. Such techniques (Mössbauer spectroscopy, nuclear magnetic resonance and perturbed angular correlations (PAC)) give information not only on the radial, but also on the angular distribution of atoms. In the past, they were widely applied to metal–metalloid and metal–metal amorphous alloys but up to now, the new class of bulk amorphous materials was not studied by these hyperfine techniques. A PAC study on these bulk metallic glasses can be very useful to characterize the short-range order of the different states of these alloys and their thermal evolution.

We present here a PAC investigation on mechanically alloyed Hf- and Zr-based alloys with the aim of contributing to the understanding of their local atomic structure.

* Corresponding author.
E-mail address: damonte@venus.fisica.unlp.edu.ar (L.C. Damonte)

2. Experimental

The amorphous $Hf_{65}Al_{7.5}Cu_{17.5}Ni_{10}$ and $Zr_{65}Al_{7.5}Cu_{17.5}Ni_{10}$ alloys were prepared by mechanical alloying of the elemental powders in a steel vial under argon atmosphere using a planetary ball mill (Retsch PM 4000). An amount of 2 at% Hf was added to the Zr-based alloy in order to get the radioactive probe for the PAC experiments. The milled powders were characterized by X-ray diffraction (XRD) (Philips PW 1050 diffractometer) using Co Kα ($\lambda = 0.17902$ nm) radiation and differential scanning calorimetry (DSC) (Perkin-Elmer DSC 7) at 40 K/min, up to a temperature of 873 K.

The samples for PAC measurements were irradiated with thermal neutrons in order to obtain the required activity of ^{181}Hf by means of the nuclear reaction ^{180}Hf$(n,\gamma)^{181}$Hf. The β decay of the ^{181}Hf isotope populates the 133–482 keV $\gamma-\gamma$ cascade in ^{181}Ta, an adequate probe for this experimental technique. The measurements were performed in a conventional apparatus [16] with two CsF scintillators providing a time resolution (full width at half maximum) of 0.8 ns. The PAC spectra were all obtained at room temperature. After subtraction of the chance coincidence back-ground, time spectra corresponding to angles 90 and 180° between detectors were combined to form the ratio

$$R(t) = 2\frac{N(180°,t) - N(90°,t)}{N(180°,t) + N(90°,t)} = A_2^{\exp}{}^t G_2(t)$$

Theoretical functions of the form $A_2G_2(t)$, folded with the measured time resolution curve, were fitted to the experimental ratio $R(t)$.

Prior to irradiation, different specimens of both samples were annealed in the calorimeter up to temperatures that characterize the different states of the alloy: relaxed amorphous, supercooled liquid, first crystallization step and second crystallization step. Additional isothermal heat treatments at 893 K, for 2 and 24 h, were performed in order to identify and characterize the final products by PAC.

The thermal evolution of the local order in the Hf-based amorphous alloys was investigated on an isothermally annealed sample at 793 K, below the first exothermic peak.

3. Results

Prior to irradiation, all the samples were analyzed by XRD. The diffractograms for the as-milled material display a broad diffuse maximum ($2\theta \cong 43°$) characteristic of an amorphous phase (Fig. 1). A similar pattern is still observed for the relaxed and supercooled liquid states. For the Hf-based alloy, some crystalline diffraction peaks of unreacted material are also observed. Those samples annealed above the second crystallization peak show several defined reflections, most of them corresponding to tetragonal Hf_2Cu, probably with some Al and/or Ni in its composition. The remaining reflections can be assigned to the intermetallic face-centered cubic (f.c.c.) Hf_2Ni. This metastable phase with a Ti_2Ni-like structure is usually stabilized by the presence of small oxygen amounts and has been observed in the crystallization of related amorphous alloys [15]. Similar findings have been reported for Zr-based quaternary amorphous alloys [17].

The as-milled samples were also characterized by scanning calorimetry displaying an endothermic reaction at low temperatures, characteristic of the glass transition (T_g), followed by two sharp exothermic crystallization peaks (T_{x1}, T_{x2}). The glass transition temperature T_g is defined as the onset temperature of the glass transition event and the crystallization temperatures T_x as the crystallization peak temperatures. From these patterns, the temperatures $T_g = 673$ K, $T_{x1} = 728$ K, $T_{x2} = 773$ K for the Zr-based alloy and $T_g = 773$ K, $T_{x1} = 823$ K, $T_{x2} = 873$ K for the Hf-based alloy were obtained. This confirms that both alloys exist in the supercooled liquid state over a wide temperature range $\Delta T_x = 50$ K (see Fig. 2).
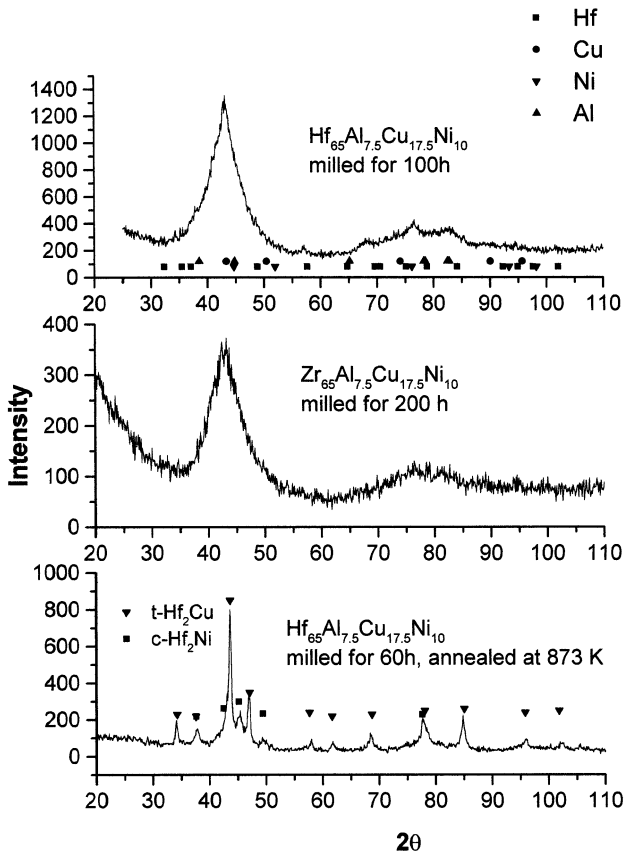

Fig. 1. XRD diffraction patterns for $Hf_{65}Al_{7.5}Cu_{17.5}Ni_{10}$ and $Zr_{65}Al_{7.5}Cu_{17.5}Ni_{10}$ (2 at% Hf).
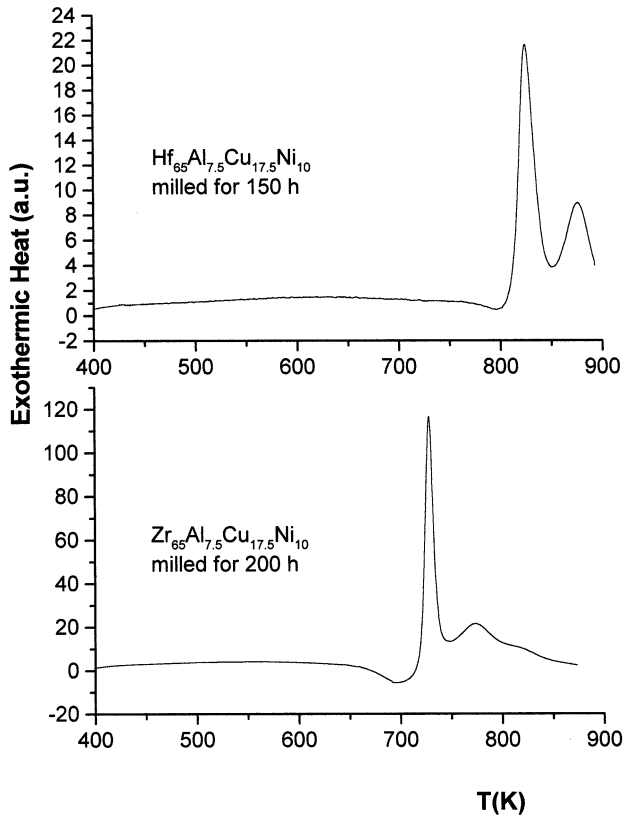
Fig. 2. DSC scans for $Hf_{65}Al_{7.5}Cu_{17.5}Ni_{10}$ and $Zr_{65}Al_{7.5}Cu_{17.5}Ni_{10}$ (2 at% Hf) (heating rate, 40 K/min).

The PAC spectra corresponding to the Hf- and Zr-based amorphous alloys together with their corresponding Fourier transforms are shown in Figs. 3 and 4, respectively. The spectra for the as-milled and the annealed at 638, 678 and 793 K Hf-based samples show a wide distribution of frequencies characteristic of an amorphous alloy [13]. The full line represents the result of least-squares fitting to the data using the perturbation factor:

$$G_2(t) = \int_0^1 d\eta \int_{-\infty}^{\infty} dV_{zz}\, P(V_{zz}, \eta) G_2^0(t; V_{zz}, \eta) \tag{1}$$

where $G_2^0(t; V_{zz}, \eta)$ is the usual quadrupole perturbation factor for polycrystalline samples. The distribution function:

$$P(V_{zz}, \eta) = \sqrt{\frac{2}{\pi}} \frac{\eta}{\Delta_{zz}} \exp[-(V_{zz} - V_{zz}^0)^2 / 2\Delta_{zz}^2] \tag{2}$$

accounts for the EFG in a dense random packing of ions [13]. The quadrupole frequency is determined by $\omega_Q = eQV_{zz}/40\eta$ (the nuclear quadrupole moment $Q = 2.51_{15}$ b [18]) and the predicted relative width $\delta = \Delta_{zz}/V_{zz} \approx 0.35$ is independent of η, the asymmetry parameter defined by $\eta = (V_{xx} - V_{yy})/V_{zz}$. In Tables 1 and 2, the resulting quadrupole parameters for Hf-and Zr-based alloys, respectively, are shown.

The as-milled state for the Hf-based alloy is characterized by a quadrupole frequency of $\omega_Q = 93_2$ Mrad/s and $\delta = 33_2\%$, and no significant changes occurred on annealing at temperatures up to 678 K. After annealing at 793 K, the average EFG strength is reduced by $\sim 10\%$ but the result still allows a description based on a dense random packing (DRP) model, which also confirms the existence of a wide range of supercooled liquid states in these alloys. Similar results were obtained for the Zr-based alloys up to a relaxing temperature of $T_a = 696$ K.

Some different results are obtained for the samples annealed up to T_{x1} (823 K for Hf-based and 720 K for Zr-based alloys). The spectra also show a wide distribution of frequencies but do not support a description based on a DRP model as a unique component. Moreover, in the case of Zr, an additional (widely distributed) interaction, comprising 18% of probe atoms, is necessary to fit the data.

In consequence, the spectra for those alloys heated to temperatures higher than T_{x1} are analyzed with two or three quadrupole interactions using the following perturbation factor:
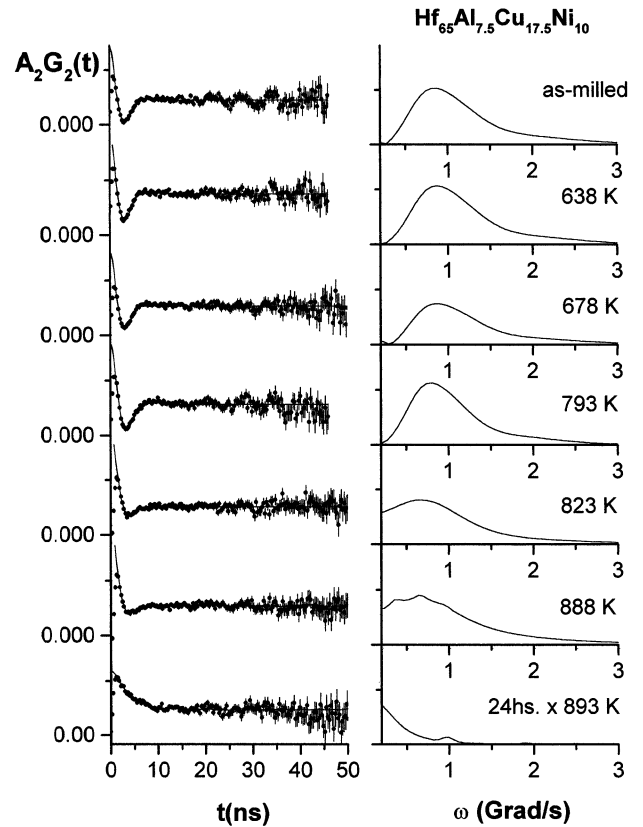

Fig. 3. PAC spectra (left) for amorphous $Hf_{65}Al_{7.5}Cu_{17.5}Ni_{10}$ for different annealing temperatures. The full line represents the result of least-squares fitting. At the right-hand side, their Fourier transforms are shown.

$Hf_{65}Al_{7.5}Cu_{17.5}Ni_{10}$

Fig. 4. PAC spectra (left) for amorphous $Zr_{65}Al_{7.5}Cu_{17.5}Ni_{10}$ (2 at% Hf) for different annealing temperatures. The full line represents the result of least-squares fitting. At the right-hand side, their Fourier transforms are shown.
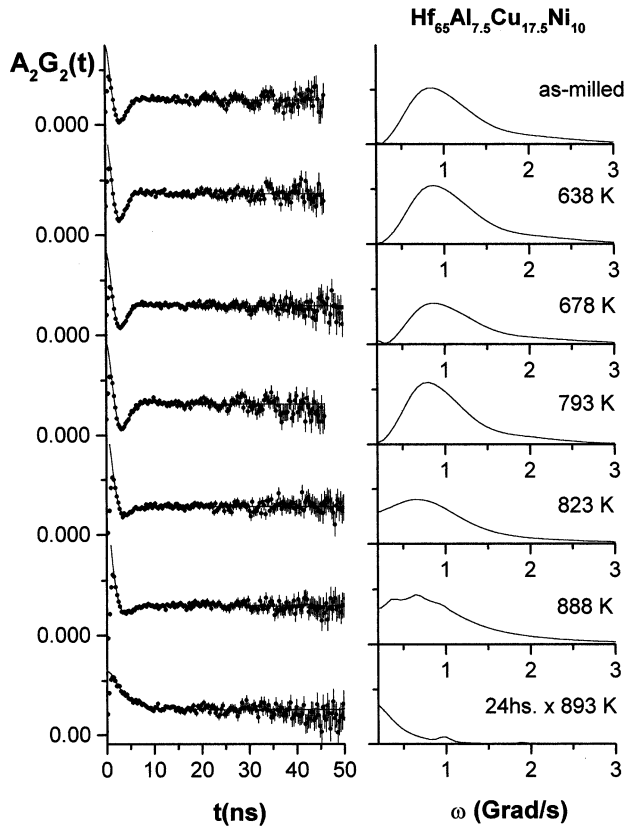
Table 1
Resulting quadrupole parameters for $Hf_{65}Al_{7.5}Cu_{17.5}Ni_{10}$[a]

$Hf_{65}Al_{7.5}Cu_{17.5}Ni_{10}$ sample	f_i	ω_{Qi}	η_i	δ_i
As-milled	100	93_2	0.66	0.33_2
638 K	100	94_2	0.66	0.31_2
678 K	100	93_1	0.66	0.32_2
793 K	100	84_2	0.66	0.33_2
823 K	100	61_5	0.78_{18}	0.71_2
848 K	98_2	74_{20}	0.53_{15}	0.69_{14}
	2.4_1	104_5	0.63_6	0.18_{60}
888 K	95_1	66_8	0.60_{12}	0.72_5
	5.2_1	112_2	0.59_2	0.09_{99}
2 h × 893 K	9_4	5.2	0.00	0.30
	4_2	117_3	0.80	0.04_{99}
	88_7	30_3	0.00	0.84_{27}
24 h × 893 K	20_7	5.2	0.00	0.30
	6_2	90_3	0.80	0.05_4
	75_8	31_2	0.00	0.61_{17}

[a] f_i (%), Population; ω_{Qi} (Mrad/s), quadrupole frequency; η_i, asymmetry parameter; δ_i, distribution.

$$G_2(t) = \sum_i f_i G_2^i(t; V_{zz}, \eta, \delta) \qquad (3)$$

where $G_2^i(t; V_{zz}, \eta, \delta)$ describes a gaussian distribution of

frequencies at a given site with relative population f_i (see Table 1).

The spectra for the samples annealed at 848 and 888 K (between the two exothermic peaks in Hf-based alloys) and at 873 K for the Zr-based alloy, are well described by one or two widely distributed frequencies using the perturbation factor (Eq. (3)). The minority component for the Hf-based alloys is better defined and its mean quadrupole frequency is close to that observed in tetragonal Hf_2Ni [15].

After the additional treatments at 893 K, on the Hf-based alloy, the results are fitted with three better-defined quadrupole interactions, which can be assigned to the intermetallic compounds expected from the stoichiometry of the alloy (equilibrium phase diagram). Two of them are those corresponding to tetragonal Hf_2Cu and Hf_2Ni, whose quadrupole parameters have been previously reported [14,15]. The third can be assigned to the intermetallic f.c.c. Hf_2Ni compound with some Al and/or Cu contained, in agreement with the X-ray pattern observed. A quadrupole frequency different from zero (as is expected for a cubic environment) may be due to the presence of those impurities in the structure.

4. Discussion

The PAC results for all the samples heated up to temperatures bellow the first exothermic peak, 793 K for Hf- and 720 K for Zr-based amorphous alloys, show that their local order is well described by a dense random packing of ions. Hence, this hyperfine technique confirms that the supercooled liquid state of these bulk metallic glasses has similar local arrangements as the initial amorphous state. For the Hf-based alloy, a 10% reduction is observed in the EFG of the super-cooled liquid state with respect to the corresponding as-milled alloy. A similar effect was previously observed [14,15], which was associated with the relaxation of the amorphous state. The mean values of the quadrupole frequencies for the initial amorphous states are consistent with the tendency observed on rapidly quenched

Table 2
Resulting quadrupole parameters for $Zr_{65}Al_{7.5}Cu_{17.5}Ni_{10}$[a]

$Zr_{65}Al_{7.5}Cu_{17.5}Ni_{10}$ sample	F_i	ω_{Qi}	η_i	δ_i
As-milled	100	80_2	0.66	0.37_1
573 K	100	84_1	0.66	0.34_1
696 K	100	81_2	0.66	0.33_1
720 K	82_{25}	70_4	0.66	0.32_7
	18_{25}	54_4	0.00	0.32_9
873 K	100	70_2	0.00	0.60_2

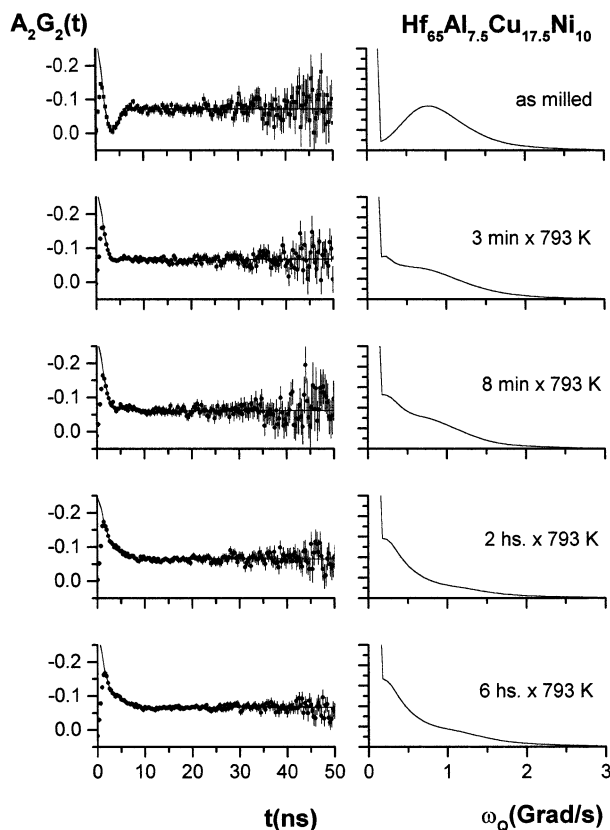[a] f_i (%), Population; ω_{Qi} (Mrad/s), quadrupole frequency; η_i, asymmetry parameter; δ_i, distribution.

Fig. 5. PAC spectra (left) for amorphous $Hf_{65}Al_{7.5}Cu_{17.5}Ni_{10}$ after isothermal annealings at 793 K. The full line represents the result of least-squares fitting. At the right-hand side, their Fourier transforms are shown.

Hf- and Zr-based amorphous alloys. We have observed that the Hf-based alloys have greater electric field gradient strength than the Zr-based ones, independent of the second component (Cu, Ni or both). In the present case, this behavior is verified: $\omega_Q = 93_2$ Mrad/s and $\omega_Q = 80_2$ Mrad/s for Hf- and Zr-based, respectively. Indeed, these values are similar to those measured on rapidly quenched binary alloys with same at% Hf or Zr [13–15].

For those samples annealed in the DSC apparatus at higher temperatures, a clear change in the local order of the alloy has occurred. This change is better appreciated on the Fourier transforms of the data (right-hand column in Figs. 3 and 4). The frequency distribution representing a DRP of ions predicts zero probability for frequency zero. This is not the same for a gaussian distribution of frequencies.

After these annealings, two frequency distributions are observed. One of these is associated with tetragonal Hf_2Ni crystalline environments, while the other represents an unknown metastable phase which, after prolonged heat treatments, evolves to the final equilibrium compounds [15]. Similar structural changes have been observed by Seidel et al. [5] in mechanically alloyed Zr–Ti–Cu–Ni samples.

The description based on wide gaussian frequency distribution remains valid for all the samples, including those heated above the second exothermic peak. Although the XRD diffractograms for the Hf-based samples annealed at 873 K show well-defined reflections, the PAC patterns do not display any single frequency pattern. It is only after a long heat treatment at 893 K that three crystalline sites are raised. A low frequency, 5 Mrad/s and $\eta = 0$, corresponds to the intermetallic compound Hf_2Cu; the second one, 90 Mrad/s and $\eta = 0.80$, identifies the tetragonal compound Hf_2Ni. Both intermetallic compounds were previously characterized by PAC [14,15]. The third component can be assigned to metastable f.c.c. Hf_2Ni compound with some Al and/or Cu contained, which evolves with temperature to a possibly stable phase Hf_6NiAl_2, or to another Hf–Al intermetallic compound. In this sense, Seidel et al. [5] claimed the formation of Zr_3Al_2 during the crystallization of Zr–Ti–Cu–Ni alloys but, recently, Eckert et al. [17] have proposed a new hexagonal phase, Zr_6NiAl_2, which, together with tetragonal Zr_2Cu, can account for all the diffraction lines. At this stage, we cannot make a unique assignment to this phase since, to our knowledge, it has not yet been characterized by PAC. The observed fraction for each component does not correspond to what is expected from the stoichiometry, so it is suspected that crystallization is not complete. Moreover, a post-irradiation X-ray diffractogram reveals the presence of these three phases, similar to that shown in Fig. 1 for the sample annealed at 873 K, discarding any radiation damage.

In order to study the crystallization process, isothermal annealings on the Hf-based relaxed sample at 793 K were made. The analysis of the PAC spectra (Fig. 5) yields two wide distributions of frequencies, one of them close to zero. A phase separation into two amorphous phases, as other authors reported [19], was not observed. In the case of phase separation, the PAC pattern would resemble two Czjzek's distributions of frequencies (Eq. (2)), as was shown in melt-spun Hf–Ni amorphous ribbons [15] after annealing above the first exothermic peak. The distribution centered at zero frequency can be associated with nuclei of crystalline Hf_2Cu, which is characterized by a low quadrupole frequency. Several authors [20,21] have reported the formation of clusters with a short-range order similar to crystalline Zr_2Cu as a first stage of crystallization in Zr–Al–Ni–Cu alloys.

The presence of various components in the alloy and the long-range diffusion of each element needed for the nucleation and growth of the equilibrium phases are the main reasons for the existence of a wide supercooled liquid region. These would also be responsible for the complicated and retarded crystallization process observed.

5. Conclusions

The as-milled and the relaxed samples show a wide distribution of electric field gradients characteristic of an amorphous phase described as a dense random packing of ions. The supercooled liquid state in both $Hf_{65}Al_{7.5}Cu_{17.5}Ni_{10}$ and $Zr_{65}Al_{7.5}Cu_{17.5}Ni_{10}$ responds to the same description. The quadrupole frequency in this state, for the Hf-based alloy, diminished 10% with respect to the initial amorphous state, indicating the effect of structural relaxation on the EFG.

The crystallization of the alloy proceeds in two steps, in agreement with DSC results. The detailed mechanism and metastable phases resulting from the crystallization process depend on the thermal history and annealing temperature. The first peak in the DSC trace is assigned to the formation of small clusters or precipitates of $CuZr_2(Hf_2)$ or metastable f.c.c. $NiZr_2(Hf_2)$, which are identified by the low frequency distribution. Another disordered phase (widely distributed) that coexists with these phases after subsequent heat treatments above the second crystallization temperature evolves to tetragonal $CuZr_2(Hf_2)$, $NiZr_2(Hf_2)$ and hexagonal $(Hf_6)Zr_6NiAl_2$ or another related phase.

Heat treatments at temperatures below the second exothermic peak lead to an important change in the local order of the alloy. The high distribution of frequencies observed in these cases may describe the formation of a disordered metastable phase. No phase separation into two amorphous phases was observed.

After very long annealings at 893 K, complete crystallization of the alloy is observed. The quadrupole interactions corresponding to tetragonal close-packed $Hf_2Ni(Zr_2Ni)$ and $Hf_2Cu(Zr_2Cu)$ compounds are well defined. A third quadrupole frequency can be associated with an intermetallic compound containing Al, Hf_3Al_2 or Hf_6NiAl_2.

Additional measurements on fully crystallized samples are needed in order to characterize all of the final equilibrium compounds.

References

[1] A. Inoue, T. Zhang, T. Masumoto, Mater. Trans. JIM 31 (1990) 425.

[2] T. Zhang, A. Inoue, T. Masumoto, Mater. Trans. JIM 32 (1991) 1005.

[3] A. Peker, W.L. Johnson, Appl. Phys. Lett. 63 (1993) 2342.

[4] W.L. Johnson, Mater. Sci. Forum 225–227 (1996) 35.

[5] M. Seidel, J. Eckert, L. Schultz, Mater. Lett. 23 (1995) 299.

[6] J. Eckert, Mater. Sci. Eng. A226–228 (1997) 364–373.

[7] A. Wiedenmann, J.-M. Liu, Solid State Commun. 100 (1996) 331.

[8] A. Wiedenmann, U. Keiderling, M.-P. Macht, H. Wollenberger, Mater. Sci. Forum 225–227 (1996) 71.

[9] J.-M. Liu, A. Wiedenmann, U. Gerold, H. Wollenberger, Mater. Sci. Forum 235–238 (1997) 523.

[10] G. Czjzek, J. Fink, F. Götz, H. Schmidt, J.M.D. Coey, J.P. Rebouillat, A. Lienard, Phys. Rev. B 23 (1981) 2513.

[11] P. Panissod, D. Aliaga Guerra, A. Amamou, J. Durand, W.L. Johnson, W.L. Carter, S.J. Poon, Phys. Rev. Lett. 44 (1980) 1465.

[12] P. Panissod, I. Bakonyi, R. Hasegawa, Phys. Rev. B 28 (1983) 2374.

[13] L. Mendoza-Zélis, L.C. Damonte, A. Bibiloni, J. Desimoni, A.R. López García, Phys. Rev. B 34 (1986) 2982.

[14] L.C. Damonte, L. Mendoza-Zélis, A.R. López García, Phys. Rev. B 39 (1989) 12492.

[15] L.C. Damonte, L.A. Mendoza-Zélis, A.R. López García, E.D. Cabanillas, Phys. Rev. B 46 (1992) 13767.

[16] A. Pasquevich, F. Sánchez, A. Bibiloni, J. Desimoni, A.R. López García, Phys. Rev. B 27 (1983) 963.

[17] J. Eckert, N. Mattern, M. Zinkevitch, M. Seidel, Mater. Trans. JIM 39 (1998) 623.

[18] N. Kaufmann, R.J. Vianden, Rev. Mod. Phys. 51 (1979) 161.

[19] U. Köster, J. Meinhardt, S. Roos, A. Rüdiger, Mater. Sci. Forum 225–227 (1996) 311.

[20] H. Schumacher, U. Herr, D. Oelgeschlaeger, A. Traverse, K. Samwer, J. Appl. Phys. 82 (1997) 155.

[21] M. Weiss, M. Moske, K. Samwer, Appl. Phys. Lett. 69 (1996) 3200.